

## A Slow Exchanging Vanadium(V) Peptide Complex: Vanadium(V)–Glycine–Tyrosine

Debbie C. Crans,<sup>\*,†</sup> Hartmut Holst,<sup>†,‡</sup> Anastasios D. Keramidas,<sup>†</sup> and Dieter Rehder<sup>\*,‡</sup>

Department of Chemistry, Colorado State University, Fort Collins, Colorado 80523-1872, and Institut für Anorganische und Angewandte Chemie der Universität, Martin-Luther-King-Platz 6, D-20146 Hamburg 13, Germany

Received December 15, 1994<sup>®</sup>

The solution structure and rate of formation for a vanadium(V)–peptide complex, vanadium(V)–glycine–tyrosine (V–Gly–Tyr), is examined. Multinuclear NMR spectroscopic studies suggest the amide nitrogen is deprotonated and chelated to the vanadium as observed in peptide complexes of Ni(II) and Cu(II). The carboxylate and the amine groups in the dipeptide also appear to be chelated to the vanadium atom. The rate law for V–Gly–Tyr complex formation suggests that the complex is generated according to two major pathways, both involving  $\text{H}_2\text{VO}_4^-$  and deprotonated glycine–tyrosine dipeptide (Gly–Tyr<sup>-</sup>), one with and one without acid catalysis. The rate constant for the first pathway was  $1.0 (\pm 0.1) \text{ M}^{-2} \text{ min}^{-1}$  ( $0.017 (\pm 0.002) \text{ M}^{-2} \text{ s}^{-1}$ ), and the rate constant for the second pathway was  $1.5 (\pm 0.1) \text{ M}^{-1} \text{ min}^{-1}$  ( $0.025 (\pm 0.003) \text{ M}^{-1} \text{ s}^{-1}$ ). The kinetics of complex formation were found to be significantly different from reported vanadate complexes such as vanadate dimer, vanadium(V)–alizarin, vanadium(V)–*N*-[tris(hydroxymethyl)methyl]glycine, vanadium(V)–EDTA, and vanadium(V)–ATPase. All of the previously studied complexes formed with  $\text{H}_3\text{O}^+$  independent rate constants of about  $10^4 \text{ M}^{-1} \text{ s}^{-1}$ . The slow rates of formation of V–Gly–Tyr imply that equilibrium in such solutions is only slowly achieved. Time dependence curves reveal that the other complexes in the reaction between vanadate and Gly–Tyr form even more slowly; however, such complexes are likely to be oxidation products since these complexes were not observed when oxygen was excluded from the solutions. Only low levels of vanadium(IV) complexes were observed in the absence or the presence of oxygen, despite significant concentrations of oxidation products. These observations are consistent with the recycling of the vanadium(IV) to vanadium(V) under the consumption of oxygen. Increasing temperatures also increase the V–Gly–Tyr concentration, however, since the vanadate monomer ( $\text{V}_1$ ) concentration increases, little variation in the formation constant is observed. The reaction of vanadate with Gly–Ser was also found to be significantly slower than the formation of vanadate esters and required incubation for more than an hour before equilibrium was achieved. It appears that complex formation between vanadate and ligands containing the peptide functionalities occurs slowly, analogous to formation of peptide complexes of Ni(II) and Cu(II).

### Introduction

The trace element vanadium can, in the form of vanadate, interact with proteins and peptides.<sup>1</sup> For some enzymes, nitrogenases and haloperoxidases, vanadium is a cofactor and for enzymes using NADP as a cofactor, NAPV, a vanadium analog of NADP, is an excellent substitute.<sup>2</sup> In general the nature of interactions of vanadium with protein is complicated by the wide range of aqueous chemistry vanadium undergoes.<sup>1,3</sup> Aqueous solutions containing vanadium(V) will generate vanadate oligoanions (including monomer ( $\text{H}_2\text{VO}_4^-$ ,  $\text{HVO}_4^{2-}$ , abbreviated  $\text{V}_1$ ), dimer ( $\text{H}_2\text{V}_2\text{O}_7^{2-}$ ,  $\text{HV}_2\text{O}_7^{3-}$ , abbreviated  $\text{V}_2$ ),

tetramer ( $\text{V}_4\text{O}_{12}^{4-}$ , abbreviated  $\text{V}_4$ ), pentamer ( $\text{V}_5\text{O}_{15}^{5-}$ , abbreviated  $\text{V}_5$ ), and decamer ( $\text{V}_{10}\text{O}_{28}^{6-}$ , abbreviated  $\text{V}_{10}$ ).<sup>3</sup> Each of these anions exhibit different affinities for proteins. The inhibitory vanadium species of phosphatases and ATPases is commonly the vanadate monomer.<sup>1,4</sup> Vanadate oligomers inhibit human seminal fluid phosphatase ( $\text{V}_2$ ),<sup>5a</sup> dehydrogenases ( $\text{V}_2$  and/or  $\text{V}_4$ ),<sup>5b–d</sup> aldolase ( $\text{V}_2$  and  $\text{V}_4$ ),<sup>5e</sup> superoxide dismutase ( $\text{V}_4$ ),<sup>5f</sup> kinases ( $\text{V}_{10}$ ),<sup>5g</sup> and phosphorylase ( $\text{V}_{10}$ ).<sup>5h</sup> In many studies the interacting vanadium species have not been specified.<sup>1</sup> The recent human clinical trials using sodium metavanadate and vanadyl sulfate as oral insulin substitutes are encouraging,<sup>6c</sup> but the mechanism and the site of action are not yet known.<sup>4,6</sup> It has been suggested that vanadate will spontaneously vanadylate a tyrosine residue in the insulin receptor leading to a vanadylated tyrosine protein or protein receptor which will then mediate a response.<sup>4,7</sup> Protein kinases and

<sup>†</sup> Colorado State University.

<sup>‡</sup> Universität Hamburg.

<sup>®</sup> Abstract published in *Advance ACS Abstracts*, March 15, 1995.

- (1) (a) Chasteen, N. D., Ed. *Vanadium in Biological Systems*; Kluwer Academic Publishers: Dordrecht, The Netherlands, 1990. (b) Rehder, D. *Angew. Chem., Int. Ed. Engl.* **1991**, 148–167. (c) Nechay, B. R.; Nanninga, L. B.; Nechay, P. S. E.; Post, R. L.; Grantham, J. J.; Macara, I. G.; Kubena, L. F.; Phillips, T. D.; Nielsen, F. H. *Fed. Proc.* **1986**, 45, 123–132. (d) Boyd, D. W.; Kustin, K. *Adv. Inorg. Biochem.* **1984**, 6, 311–365. (e) Crans, D. C. *Comments Inorg. Chem.* **1994**, 16, 1–33. (f) Crans, D. C. *Met. Ions Biol.* **1995**, 31, 147–209.
- (2) (a) Robson, R. L.; Eady, R. R.; Richardson, T. H.; Miller, R. W.; Hawkins, M.; Postgate, J. R. *Nature (London)* **1986**, 322, 388–390. (b) Wever, R.; Kustin, K. *Adv. Inorg. Chem.* **1990**, 35, 81–115. (c) Crans, D. C.; Simone, C. M.; Blanchard, J. S. *J. Am. Chem. Soc.* **1992**, 114, 4926–4928. (d) Crans, D. C.; Marshman, R. W.; Nielsen, R.; Felty, I. *J. Org. Chem.* **1993**, 58, 2244–2252.
- (3) (a) Pope, M. T. *Heteropoly and Isopoly Oxometalates*; Springer-Verlag: New York, 1983. (b) Crans, D. C. *Comments Inorg. Chem.* **1994**, 16, 35–76.

(4) (a) Gresser, M. J.; Tracey, A. S.; Stankiewicz, P. J. *Adv. Protein Phosphatases* **1987**, 4, 35–57. (b) Chasteen, N. D. *Struct. Bonding (Berlin)* **1983**, 53, 105–38.

(5) (a) Crans, D. C.; Simone, C. M.; Saha, A. K.; Glew, R. H. *Biochem. Biophys. Res. Commun.* **1989**, 165, 246–250. (b) Crans, D. C.; Schelble, S. M. *Biochemistry* **1990**, 29, 6698–706. (c) Crans, D. C.; Simone, C. M. *Biochemistry* **1991**, 30, 6734–6741. (d) Crans, D. C.; Willging, E. M.; Butler, S. R. *J. Am. Chem. Soc.* **1990**, 112, 427–432. (e) Crans, D. C.; Sudhakar, K.; Zamborelli, T. J. *Biochemistry*, **1992**, 31, 6812–6821. (f) Wittenkeller, L.; Abrahama, A.; Ramasamy, R.; Mota de Freitas, D. M.; Theisen, L. A.; Crans, D. C. *J. Am. Chem. Soc.* **1991**, 113, 7872–7881. (g) Boyd, D. W.; Kustin, K.; Niwa, M. *Biochim. Biophys. Acta* **1985**, 827, 472–475. (h) Soman, G.; Chang, Y. C.; Graves, D. J. *Biochemistry* **1983**, 22, 4994–5000.

phosphatases are activated or inhibited in the presence of vanadate, and it has been proposed that these phenomena may be related to whether the enzymes contain tyrosine or serine/threonine residues that are phosphorylated.<sup>4</sup> Since the reaction between vanadate and Gly—Ser has been examined in detail,<sup>8</sup> it is of particular interest to compare the interaction of vanadate with tyrosine containing peptides.

The reaction of vanadate with selected amino acids, peptides, proteins, and related compounds has been reported.<sup>8–13</sup> The complexes formed between vanadate and several amino acids, small peptides, or related compounds were studied using <sup>51</sup>V NMR spectroscopy and structures have been suggested for these complexes.<sup>9,10,12a,14</sup> The reaction between vanadate and dipeptides such as Gly—Gly, Gly—Ser, Gly—Val, Gly—Asp, and Leu—Leu form a major complex at approximately -507 ppm by <sup>51</sup>V NMR. The free amino and carboxylate groups as well as the amide nitrogen in the dipeptide is presumably involved in the interaction with vanadate. If any of these three groups are inaccessible, this complex will not form.<sup>8,9</sup> The amide group in all these complexes chelates to the vanadium, although the amide functionality, in place of an amine functionality, decreases the stability of the related triethanolamine vanadate complexes.<sup>13</sup> A minor complex at about -560 ppm will also form with some peptides; this complex probably involves complexation between vanadate and the carboxylate group of the peptide, since such a complex does not form when the ligand is esterified.<sup>8</sup> A recent report of a vanadium(V)—amide complex has demonstrated that these types of complexes can form and, in some cases, may enjoy a five-coordinate environment.<sup>12b</sup> The reaction between vanadate and serine is more complicated because the serine group can complex through its side chain.<sup>8</sup>

Formation rates of vanadium-containing complexes have only been reported for a few complexes.<sup>15–18</sup> The reaction of vanadate with hydroxyl groups such as in ethanol is completed in milliseconds,<sup>15</sup> and the reaction of vanadate with phenolic groups is on the same order of magnitude in aqueous solution at 25 °C.<sup>17</sup> Multidentate ligands such as alizarin,<sup>17</sup> EDTA<sup>17</sup> and Tricine (*N*-[tris(hydroxymethyl)methyl]glycine)<sup>16</sup> will form complexes with vanadate with a second order rate constant about 10<sup>4</sup> M<sup>-1</sup> s<sup>-1</sup>. A similar rate constant is observed when vanadate interacts with an enzyme such as ATPase.<sup>18</sup> Slower reaction

rates have been observed for vanadate interactions with enzymes such as aldolase<sup>19</sup> and the second order rate constant for the reaction between vanadate and ethanol.<sup>15</sup> No information is available for the rates of vanadate—peptide complex formation; such rates may be dependent on the specific peptide sequence.

Reactions of simple peptides with other metal ions such as Cu(II) and Ni(II) form complexes with deprotonated amide nitrogen atoms.<sup>20–24</sup> Protonation reactions of Ni(II) and Cu(II) complexes have rate constants on the order of 10<sup>4</sup>–10<sup>7</sup> M<sup>-1</sup> s<sup>-1</sup> rather than the approximate 10<sup>10</sup> M<sup>-1</sup> s<sup>-1</sup> as expected for diffusion-controlled reactions in aqueous solution at ambient temperature.<sup>25</sup> It has been proposed that these slow rates are related to the metal—N(peptide) group since this is the group often displaced in protonation leading to extensive structural and electronic rearrangements within the complex.<sup>21</sup> The amide nitrogen can protonate when still coordinated to the metal, and this will greatly weaken the nitrogen's donor ability forcing the complex to dissociate (at least one ligand). If, on the other hand, the metal—N(peptide) bond is cleaved in the complex before protonation,<sup>26</sup> the N(peptide) will immediately abstract a proton from water and produce a poor ligand to the metal. The —CONH— (or in deprotonated form —CON<sup>-</sup>) functionality in the peptide does not, therefore, come on and off in a complex, as with other chelating functionalities.<sup>20b</sup> Kinetics of the Cu(II) and Ni(II) peptide complexes have in the past been described, whereas no information is available on the kinetics of vanadate—peptide complexes.

The thermodynamics and kinetics of the reaction of vanadate with Gly—Tyr was examined using multinuclear NMR spectroscopy. We specifically chose to study the reaction of vanadate with Gly—Tyr to compare tyrosine—vanadate derivatives with the serine—vanadate complexes.<sup>8</sup> Not only did we find that the vanadium(V)—Gly—Tyr complex forms more slowly than vanadate complexes with alcohols, carboxylates and amines, but also we found that the V—Gly—Ser complex forms slowly as well. In addition, a complex that forms in solutions after longer incubation times was characterized as an oxidation product of the ligand which then forms a complex observable by <sup>51</sup>V NMR spectroscopy. We examined the spectroscopic properties and assigned a structural arrangement to the vanadium(V)—peptide complex consistent with the slow rate of complex formation. We conclude that peptides as ligands offer a great potential for generation of hydrolytically stable vanadium(V) compounds.

## Experimental Section

**Reagents.** The reagents were all reagent grade and used without purification unless specified. The water was distilled and deionized. The vanadium solutions were prepared from either sodium metavanadate or sodium orthovanadate, and pale yellow stock solutions were obtained.

- (6) (a) Posner, B. I.; Faure, R.; Burgess, J. W.; Bevan, A. P.; Lachance, D.; Zhang-Sun, G.; Fantus, I. G.; Ng, J. B.; Hall, D. A.; Soo Lum, B.; Shaver, A. *J. Biol. Chem.* **1994**, *269*, 4596–4604. (b) McNeill, J. H.; Yuen, V. G.; Hoveyda, H. R.; Orvig, C. *J. Med. Chem.* **1992**, *35*, 1489–1491. (c) Symposium Proceedings of the "Vanadium" Symposium, July 28–30, 1994: Biochemistry, Physiology and Therapy of Vanadium in Diabetes, appearing as a special volume of *Mol. Cell. Biochem.*, in press.
- (7) Tracey, A. S.; Gresser, M. J. *Proc. Natl. Acad. Sci. U.S.A.* **1986**, *83*, 609–613.
- (8) Jaswal, J. S.; Tracey, A. S. *Can. J. Chem.* **1991**, *69*, 1600–1607.
- (9) Rehder, D. *Inorg. Chem.* **1988**, *27*, 4312–4316.
- (10) Crans, D. C.; Bunch, R. L.; Theisen, L. A. *J. Am. Chem. Soc.* **1989**, *111*, 7597–7607.
- (11) (a) Knüttel, K.; Müller, A.; Rehder, D.; Vilter, H.; Wittneben, V. *FEBS Lett.* **1992**, *302*, 11–14. (b) Rehder, D.; Holst, H.; Priebisch, W.; Vilter, H. *J. Inorg. Biochem.* **1991**, *41*, 171–178.
- (12) (a) Vergopoulos, V.; Priebisch, W.; Fritzsche, M.; Rehder, D. *Inorg. Chem.* **1993**, *32*, 1844–1849. (b) Cornman, C. R.; Geiser-Bush, K. M.; Singh, P. *Inorg. Chem.* **1994**, *33*, 4621–4622.
- (13) Crans, D. C.; Shin, P. K. *Inorg. Chem.* **1988**, *27*, 1797–1806.
- (14) Tracey, A. S.; Gresser, M. J. *Inorg. Chem.* **1988**, *27*, 1269–1275.
- (15) (a) Gresser, M. J.; Tracey, A. S. *J. Am. Chem. Soc.* **1985**, *107*, 4215–4220. (b) Crans, D. C.; Schelblin, S. M.; Theisen, L. A. *J. Org. Chem.* **1991**, *56*, 1266–1274.
- (16) Crans, D. C.; Ehde, P. M.; Shin, P. K.; Pettersson, L. *J. Am. Chem. Soc.* **1991**, *113*, 3728–3736.
- (17) Kustin, K.; Toppen, D. L. *J. Am. Chem. Soc.* **1973**, *95*, 3564–3568.
- (18) Cantley, L. C.; Josephson, L.; Gelles, J.; Cantley, L. G. in *Na, K-ATPase Structure and Kinetics*; Skou, J. C., Nørby, J. G., Eds.; Academic Press: London, 1979; pp 181–191.

- (19) (a) Crans, D. C.; Sudhakar, K.; Felty, I. Manuscript in preparation. (b) Crans, D. C.; Simone, C. M.; Holz, R. C.; Que, L., Jr. *Biochemistry* **1992**, *31*, 11731–11739.
- (20) (a) Sigel, H.; Martin, R. B. *Chem. Rev.* **1982**, *82*, 385–426. (b) Margerum, D. W.; Dukes, G. R. *Met. Ions Biol. Syst.* **1974**, *1*, 157–212.
- (21) Pagenkopf, G. K.; Margerum, D. W. *J. Am. Chem. Soc.* **1968**, *90*, 6963–6967.
- (22) Pagenkopf, G. K.; Margerum, D. W. *J. Am. Chem. Soc.* **1968**, *90*, 501–502.
- (23) Billo, E. J.; Margerum, D. W. *J. Am. Chem. Soc.* **1970**, *92*, 6811–6818.
- (24) Zuberbühler, A.; Kaden, Th. *Helv. Chim. Acta.* **1972**, *55*, 623–629.
- (25) Eigen, M. *Angew. Chem., Int. Ed. Engl.* **1964**, *3*, 1–19.
- (26) (a) Kim, M. K.; Martell, A. E. *Biochemistry* **1964**, *3*, 1169–1174. (b) Kim, M. K.; Martell, A. E. *J. Am. Chem. Soc.* **1966**, *88*, 914–918. (c) Kim, M. K.; Martell, A. E. *J. Am. Chem. Soc.* **1969**, *91*, 872–878. (d) Bryce, G. F.; Gurd, F. R. N. *J. Biol. Chem.* **1966**, *241*, 1439–1448.

The 0.400 and 0.300 M stock solutions were stored at 4 °C and protected from light. Stock solutions were not prepared from the peptides given the tendency of such solutions to support growth of microorganisms. The peptides were added as solids directly to each sample. Samples containing vanadate and peptides, when incubated at ambient and higher temperature, were kept under a Parafilm cover to reduce microorganism growth and evaporation. Only in a few cases upon extended incubation times were unusual coloration or smells noticed, and such samples were discarded without further analysis.

**Preparation of [<sup>15</sup>N]-Gly-Tyr.** First, 1.3 g (5.5 mmol) of Tyr-OtBu was dissolved in 20 mL of CH<sub>2</sub>Cl<sub>2</sub> and treated with 1.2 g (5.7 mmol) of dicyclohexylcarbodiimide (DCC) dissolved in 5 mL of CH<sub>2</sub>Cl<sub>2</sub>. The BOC-[<sup>15</sup>N]-Gly (0.84 g, 5.1 mmol), prepared according to standard procedures from [<sup>15</sup>N]-Gly (Isotec, Inc.; 98% isotopically pure), was then added to the solution containing Tyr-OtBu. After overnight stirring, the mixture was concentrated in vacuo. The removal of unreacted amino acids and dicyclohexylurea from the syrup was carried out by column chromatography (50 g of silica gel) using ethyl acetate as elutant. Removal of the ethyl acetate in vacuo yielded a white, foamy powder of BOC-[<sup>15</sup>N]-Gly-Tyr-OtBu. The yield was 1.8 g (4.6 mmol; 90%), <sup>1</sup>H NMR (250 MHz, CDCl<sub>3</sub>): 1.4 (2 singlets 9H each, BOC and tBu), 3.0 (d, 2H, PhCH<sub>2</sub>), 3.7 (t, 2H, CH<sub>2</sub>), 4.7 (m, 1H, CH), 6.8 (m, 4H, Ph).

Removal of the protecting groups was carried out as follows: The dipeptide (1.7 g, 4.3 mmol) was stirred for 30 min at room temperature with 80 mL of formic acid. The formic acid was removed in vacuo on a water bath at 30 °C. The resulting powder contained one major component by thin-layer chromatography. This material was stirred for 30 min in trifluoroacetic acid before the acid was removed in vacuo. The remaining syrup was washed several times with ether, and a small amount of water was added. Undissolved products were filtered off, and 1 M NaOH was added to the aqueous solution to pH 6. Acetone (100 mL) was added to the suspension, and the mixture was left standing overnight. During this time, unprotected [<sup>15</sup>N]-Gly-Tyr precipitated in the form of a microcrystalline, white powder. The yield was 0.48 g (2.0 mmol, 46%). <sup>1</sup>H NMR (250 MHz, D<sub>2</sub>O): 3.0 (doublet of doublets of doublets, 2H, PhCH<sub>2</sub>), 3.8 (q, 2H, CH<sub>2</sub>), 4.4 (q, 1H, CH), 7.05 (m, 4H, Ph).

**Preparation of Gly-[<sup>15</sup>N]-Tyr.** L-(<sup>15</sup>N)-Tyr (1.00 g, 5.48 mmol) was dissolved in 8.4 mL of dioxane in a 50 mL Sovirel tube and treated with 4-toluenesulfonic acid monohydrate (2.00 g, 10.5 mmol). Into this mixture was condensed 9 mL of isobutene after cooling to -15 °C. The tube was sealed and the contents stirred at ambient temperature for 20 h. The solution was then hydrolyzed at 0 °C after additions of a mixture of 33 mL of ethyl acetate, 33 mL of water and 1.7 mL of 5 M NaOH. The pH was adjusted to 9.1 and [<sup>15</sup>N]-Tyr-OtBu was extracted with three 10 mL portions of ether. After the reaction mixture was dried with MgSO<sub>4</sub>, the solvent was evaporated and the residue dried in vacuo. The yield was 770 mg (3.23 mmol, 58.9%).

[<sup>15</sup>N]-Tyr-OtBu (500 mg, 2.10 mmol) and 362 mg (2.10 mmol) of BOC-Gly were dissolved in 15 mL of absolute CH<sub>2</sub>Cl<sub>2</sub> and treated with 433 mg DCC (2.10 mmol; 1 equiv). The solution was stored at 2 °C overnight. The precipitate was filtered off, the solvent removed in vacuo and the BOC-Gly-[<sup>15</sup>N]-Gly-OtBu residue dried to form a white, foamy solid. The yield was 696 mg (1.76 mmol, 83.8%). <sup>1</sup>H NMR (250 MHz, CDCl<sub>3</sub>): 1.44 (2 s, 9H each, BOC and tBu), 3.02 (doublet of doublets of doublets, 2H, PhCH<sub>2</sub>), 3.68 (t, 2H, CH<sub>2</sub>), 4.72 (m, 1H, CH), 6.79 (m, 4H, Ph).

BOC-Gly-[<sup>15</sup>N]-Tyr-OtBu (250 mg, 0.635 mmol) was stirred in 7.5 mL of trifluoroacetic acid for 30 min and concentrated to an oil. This was washed with absolute ether and the residue treated with a few mL of water. Undissolved material was removed by filtration and the filtrate adjusted to pH 6 with 1 M NaOH. Addition of 15 mL of acetone and storage overnight afforded Gly-[<sup>15</sup>N]-Tyr in the form of white crystals. The yield was 91 mg (0.33 mmol, 86%). <sup>1</sup>H NMR (250 MHz, D<sub>2</sub>O): 2.96 (doublet of doublets of doublets, 2 H, PhCH<sub>2</sub>), 3.81 (q, 2H, CH<sub>2</sub>), 4.43 (q, 1H, CH), 7.05 (m, 4H, Ph).

**<sup>51</sup>V NMR Samples of V-Gly-Tyr (without Heating in the Presence of Oxygen).** All the 4.00 (±0.02) mL samples, containing the desired vanadate and Gly-Tyr concentration, were prepared in a similar fashion. A representative sample containing 20 mM vanadate

and 60 mM Gly-Tyr at pH 7.10 (±0.05) is described. Solid dipeptide (0.0657 g, 0.240 mmol) Gly-Tyr·2H<sub>2</sub>O was added to a 5 mL vial and 2.000 mL of D<sub>2</sub>O and 1.800 mL of H<sub>2</sub>O were added under magnetic stirring. The pH was adjusted to 6.75 (±0.05) and 0.200 mL of 0.400 M sodium vanadate (pH 8.95) was added. The pH was then measured and adjusted to the final value of 7.10 (±0.05) with 13 M NaOH which was added by means of a microliter Eppendorf pipet. A maximum volume of 0.015 mL NaOH was added and does not represent a significant perturbation of the 4.00 mL sample. The time of preparation was noted, and the vial was covered with Parafilm. If the pH of the sample was neutral, the NMR was recorded at the earliest 24 h after sample preparation. If the sample had a pH at 8 or above, the sample was incubated for 5 to 10 days before the <sup>51</sup>V NMR spectra were recorded. The pH was periodically checked and adjusted if changes occurred during the incubation period.

The samples used for time-dependence studies were prepared as described above, incubated for the desired time, and then transferred to the NMR spectrometer 10 min before the indicated time, and spectra were recorded (with 5 min setup and 10 min accumulation, the indicated time would be 10 min). Since the reaction continues to occur while the <sup>51</sup>V NMR is being recorded, the observed spectrum will reflect an average concentration at the 10 min time point.

**<sup>51</sup>V NMR Samples of V-Gly-Tyr (Using Heat Treatments in the Presence of Oxygen).** All of the 3.00 (±0.02) mL samples in this series were prepared in a similar fashion and contained the desired vanadate and Gly-Tyr concentrations. A representative sample containing 10 mM vanadate and 50 mM peptide at pH 7.20 (±0.05) is described. Solid Gly-Tyr·2H<sub>2</sub>O (0.0411 g, 0.150 mmol) was added to a 5 mL vial, and 2.900 mL of a stock solution containing H<sub>2</sub>O and D<sub>2</sub>O in a 2 to 1 volume ratio was added to the peptide. After the Gly-Tyr had dissolved, 0.100 mL of 0.300 M sodium vanadate (pH adjusted to 8.55) was added to the solution and the pH was adjusted to 7.25 (±0.05) using 11 M NaOH and 2.5 M NaOH. No more than 0.010 mL of base was needed to adjust the pH. The solution was covered with Parafilm and heated to 40 °C for 5 h. After the sample had reached room temperature, the pH was readjusted to 7.25 (±0.05) by adding 2.5 M NaOH and was again heated at 40 °C for 5 h the following day. The samples were heated three times before pH was stabilized and then incubated for 5 days or longer at the desired temperature before recording the <sup>51</sup>V NMR spectrum.

**Preparation of the V-Gly-Tyr Complex Sample in the Absence of Oxygen.** The solid Gly-Tyr (0.164 g, 0.600 mmol) and NaVO<sub>3</sub> (0.0244 g, 0.200 mmol) was added in a Schlenk flask, which was prefilled with nitrogen, and marked to indicate the 10 mL volume. Deionized water (200 mL) was placed in a second Schlenk flask with nitrogen flushing through while the water was heated to the boiling point. The water was boiled for about 1.5 h under a stream of nitrogen. The water was maintained under this flow of nitrogen while cooling. A new rubber stopper was placed on both Schlenk flasks, and the solution was transferred by canula from one flask to the flask containing the solid until the 10 mL-mark was reached. The pH was checked directly in the Schlenk flask with a long thin pH electrode under a stream of nitrogen. The pH was adjusted with zero to two drops of deoxygenated 5.0 M NaOH to pH 7.1 (±0.05) and 8.1 (±0.05), respectively. The solution in the Schlenk flask was bubbled with nitrogen for 15 min daily. The sample was then left at ambient temperature, protected from direct light, until it was time to record the EPR and NMR spectra. At this time, the EPR (or NMR) tube was flushed with nitrogen and sealed with a stopper. The sample was transferred by canula from the Schlenk flask to the EPR (or NMR) tube, and the spectrum was recorded. After the spectrum was recorded, the sample was poured from the EPR tube to a test tube for checking the pH. When additional time points were obtained, the EPR (NMR) tube was again filled with nitrogen and the process repeated in filling the EPR tube from the sample in the Schlenk flask.

**Incubations.** The samples were incubated at ambient temperatures (296 ± 2 K) in a test tube rack. At higher temperatures, the samples were fixed in styrofoam racks in a variable temperature water bath and incubated at 44 (±0.2) °C. When the sample was to be examined by NMR spectroscopy at variable temperatures, the sample was removed from the temperature bath immediately before subjecting it to NMR analysis.

**Table 1.** Equilibrium Constants for Reactions 1–5 Determining  $K_{eq}$ ,<sup>a</sup>  $K_{12}$ ,  $K_{14}$ , and  $K_{24}$ <sup>b</sup>

$K_{eq}/M^{-1}$	$K_{12}/M^{-1}$	$K_{14}/M^{-3}$	$K_{24}/M^{-1}$	method
120 ( $\pm 10$ ) <sup>a</sup>	360 ( $\pm 10$ )	$5.2 (\pm 0.1) \times 10^8$	$4100 \pm 200$	295 K incubation for 48 h, pH 7.25
150 ( $\pm 10$ ) <sup>a</sup>	370 ( $\pm 10$ )	$5.2 (\pm 0.1) \times 10^8$	$3800 \pm 300$	pH 7.25, prepared by heating and incubation cycles for 5 days at ambient temperature
130 ( $\pm 10$ ) <sup>a</sup>	95 ( $\pm 8$ )	$7.0 (\pm 0.1) \times 10^6$	$680 \pm 30$	320 K, incubation for 6 h, pH 7.25

<sup>a</sup>  $K_{eq} = [V\text{-Gly-Tyr}]/[V_1][\text{Gly-Tyr}]$ . <sup>b</sup> The errors indicated exceed those of a 95% confidence limit and correspond to a 99% confidence limit.

**<sup>51</sup>V NMR Spectroscopy.**<sup>27</sup> The <sup>51</sup>V NMR spectra were recorded at 52 MHz on a <sup>1</sup>H 200 MHz Bruker WPSY spectrometer (4.7 T), at 79 MHz on a <sup>1</sup>H 300 MHz Bruker ACP spectrometer (7.0 T), and at 131 MHz on a <sup>1</sup>H 500 MHz AM spectrometer (11.7 T). The instruments are equipped with a temperature control unit, and we estimate the temperature was constant, with a maximum error of  $\pm 1.5$  °C. With the exception of the VT experiments, the samples were recorded at 300 K to ensure constant temperatures. We used slightly elevated temperatures because, particularly in the kinetic runs, slight temperature variation causes significant changes in the rates of complex formation. The temperature unit in the NMR spectrometer was calibrated using a methanol sample.<sup>28a</sup> We typically used spectral widths between 8 and 11 KHz, a 90° pulse angle, an accumulation time of 0.1 to 0.2 s, and no relaxation delay. No differences in the integrations were observed if relaxation delays were applied. The chemical shifts were recorded relative to the external standard VOCl<sub>3</sub> at 0 ppm.

**<sup>13</sup>C NMR Spectroscopy.** The <sup>13</sup>C{<sup>1</sup>H} NMR spectra were recorded at 75 MHz on a <sup>1</sup>H 300 MHz Bruker ACP NMR spectrometer. The spectra were recorded at 296, 300, 310, and 320 K ( $\pm 1.5$  K). Accumulation of 6000–11500 transients with the use of spectral widths between 13 and 15 KHz, a 35° pulse angle, an accumulation time of 0.82 s, and a relaxation delay of 1 min were used when recording the spectra. The chemical shifts are reported with respect to an external standard (DSS).

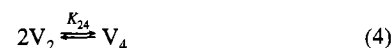
**<sup>15</sup>N NMR Spectroscopy.** The <sup>15</sup>N NMR spectra were recorded at 30.4 MHz on a <sup>1</sup>H 300 MHz Bruker ACP NMR spectrometer. The spectra were recorded at 298 K using about 3000 transients, a relaxation delay of 10 s, a pulse angle of about 45°, and a spectral width of 25 KHz. The spectra were referenced against CH<sub>3</sub>NO<sub>2</sub> (neat) as an external reference and are recorded relative to liquid NH<sub>3</sub> ( $\delta = 0$  ppm).

**EPR Spectroscopy.** The EPR spectra were recorded on a Bruker ESP 300 spectrometer in frozen aqueous solutions at 140 K in 4 mm o.d. quartz tubes. The spectrometer was operating at X-band (9.46 GHz) with a microwave power of 200 mW. Furthermore, we used a modulation frequency of 100 KHz, a modulation amplitude of 7.95 G, a time constant of 20.48 ms, a conversion time of 81.92 ms and a receiver gain of  $4 \times 10^5$ . The spectrometer was calibrated using a powder sample of 2,2-bis(4-*tert*-octylphenyl)-1-picrylhydrazyl (DPPH,  $g = 2.0037$ ).

The concentration of the VO<sup>2+</sup>–Gly–Tyr complex was determined using the area under the EPR absorption curve as described previously.<sup>28b</sup> For a first-derivative line, the area (*A*) is related to the peak-to-peak line width ( $\Delta H_{pp}$ ) and the full first-derivative signal height (*h*) by  $A = kh\Delta H_{pp}^2$ . In this relationship  $k = 1.81$  and  $0.566$  for Lorentzian and Gaussian line-shape functions, respectively. Since there is no change in line shape and width, the concentration of V<sup>4+</sup> is directly proportional to the signal height,<sup>28b</sup> and it was not necessary to use Lorentzian and Gaussian simulations to obtain the concentration in the spectrum. The quantization was confirmed by integrating (using the Bruker software) the first derivative spectrum. Known concentrations of VO<sup>2+</sup>–Gly–Tyr complex at neutral pH were used to confirm the quantization by these methods. The indicated error estimates are standard deviations of four different quantizations.

**Analysis.** Vanadate rapidly<sup>28c</sup> forms oligomers (vanadate monomer (V<sub>1</sub>), dimer (V<sub>2</sub>), tetramer (V<sub>4</sub>), and pentamer (V<sub>5</sub>)) in aqueous solutions

at neutral pH. In the millimolar concentration range, the oligomers are in equilibrium and satisfy eqs 1–4. In concentration ranges where V<sub>1</sub> and V<sub>2</sub> molefractions from the integrations of the <sup>51</sup>V NMR spectra are less accurately determined, the V<sub>4</sub> molefraction and eqs 1, 2, and 4 are used to accurately calculate the V<sub>1</sub> and V<sub>2</sub> concentrations.<sup>8,10</sup>



The H<sup>+</sup>-dependent equilibrium constants are calculated using Cricket Graph, and correlation coefficients were typically above 0.99 and never below 0.98 for indicated fits. These equilibrium constants are summarized in Table 1 for the different series studied in this work.

**Uncertainties.** The V<sub>1</sub>, V<sub>2</sub>, V<sub>4</sub>, and V<sub>5</sub> concentrations were measured within a few percent in duplicate experiments. The accuracy of experiments is sensitive to the temperature at which the experiments were carried out. The temperature is maintained within  $\pm 1.5$  °C for the NMR studies,  $\pm 0.2$  °C in the incubations in the temperature bath, and  $\pm 2$  °C in the ambient temperature incubations. Every sample was determined twice either by recording the NMR after further incubation or by recording the <sup>51</sup>V NMR of duplicate samples. The major vanadate–peptide resonance is fairly broad, and as such more difficult to measure than the oligomers; the complex concentrations were, however, measured within 5% in duplicate or repeated experiments. We carried out experiments at different NMR fields to verify the observed number of resonances in the spectra.

The uncertainties in the experiments given throughout the paper, unless specified otherwise, reflect standard deviation of 95% confidence limit. The error analysis was carried out using the statistical analysis program Statworks.

## Results and Discussion

**Reaction of Vanadate with Gly–Tyr.** The reaction of vanadate with Gly–Tyr at pH 7.1 results in the formation of a complex at  $-509$  ppm; as we will show below the formation of this complex is slow, and extended incubation periods are required for the reaction to reach equilibrium. By varying peptide and vanadate concentrations and recording the <sup>51</sup>V NMR spectra of equilibrated solutions, one can deduce the stoichiometry of the complex from reactions 5–8 as described previously for several vanadium(V)–peptide complexes.<sup>8,9,12</sup> As shown here, eqs 5–8 only define the stoichiometry with respect to the vanadium atom and the peptide; no information on loss of water or loss of H<sup>+</sup> is provided.

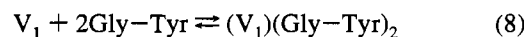
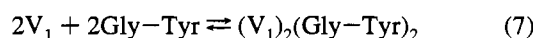
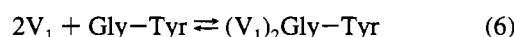
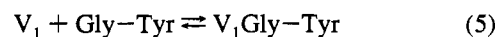
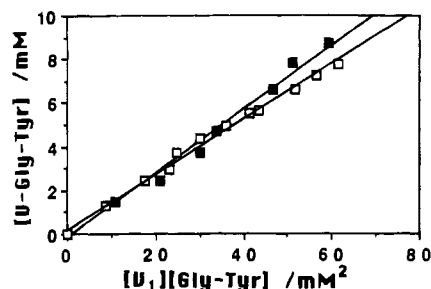
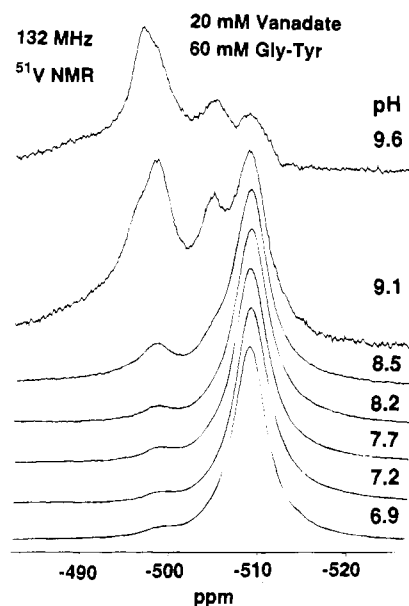


Figure 1 shows the relationship of complex concentration to

- (27) (a) Heath, E.; Howarth, O. W. *J. Chem. Soc. Dalton* **1981**, 1105–1110. (b) Rehder, D. *Bull. Magn. Reson.* **1982**, *4*, 33–83. (c) Howarth, O. W. *Prog. Nucl. Magn. Reson. Spectrosc.* **1990**, *22*, 453–483. (d) Rehder, D. in *Transition Metal Nuclear Magnetic Resonance*, Pregosin, P. S., Ed.; Elsevier: Amsterdam, **1991**; pp 1–48.
- (28) (a) van Geet, A. L. *Anal. Chem.* **1970**, *42*, 679–680. (b) Chasteen, N. D. *Structure and Bonding*; Clarke, M. J. et al., Eds.; Springer-Verlag: New York, **1983**, pp 105–138. (c) Crans, D. C.; Rithner, C. D.; Theisen, L. A. *J. Am. Chem. Soc.* **1990**, *112*, 2901–2908.



**Figure 1.** Plot of the concentration of vanadium(V)-Gly-Tyr complex as a function of  $V_1$  concentration multiplied with Gly-Tyr concentration using heat treatments (■) and no heat treatments (□). Series were conducted using constant peptide concentrations (□) and constant  $V_{tot}$  concentration (■); analogous results are obtained with constant  $V_{tot}$  with no heat treatments and with constant peptide concentration with heat treatments (data not shown).

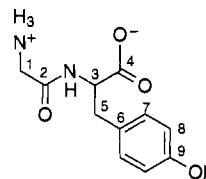


**Figure 2.** 132 MHz  $^{51}\text{V}$  NMR spectra of a solution containing 20 mM vanadate and 60 mM Gly-Tyr are shown at the indicated pH.

the product of  $V_1$  concentration and peptide concentrations according to reaction 5. In one series of experiments, samples were prepared at ambient temperature and then equilibrated. In another series the samples were subjected to various heating cycles followed by equilibration at ambient temperatures. The results by both methods are shown in Figure 1 and tabulated in Table 1.  $^{51}\text{V}$  NMR describes the average form of monomeric vanadate [ $V_1$ ], and represents the sum of the concentrations of the various forms of monomeric vanadate. Analogously, Gly-Tyr represents the sum of the three forms of dipeptide. The relationships described by reactions 6–8 were also tested, but did not give acceptable linear fits. We conclude that the complex at  $-509$  ppm is a 1:1 complex which is in agreement with observations made in reaction of vanadate with other dipeptides.<sup>8,9,12</sup> A signal with a chemical shift close to that of  $V_1$  is also observed. At pH 7.1, 7.6, 8.4 and 9.0, the  $^{51}\text{V}$  chemical shift of this signal is  $-558$  ppm,  $-552$  ppm,  $-548$  ppm and  $-537$  ppm. This signal is presumably a 1:1 complex between vanadate and the phenol group in the tyrosine. A monoester was reported to form between vanadate and tyrosine and had a similar  $^{51}\text{V}$  NMR shift.<sup>7</sup>

The formation of complex at  $-509$  ppm is shown in Figure 2 as a function of pH. An additional major species emerges at  $-498$  ppm. At pH 7 this complex is not visible at 51 or 79 MHz but is easily observed at 132 MHz. New complexes

**Table 2.**  $^{13}\text{C}$  NMR Chemical Shifts for Gly-Tyr and the Vanadate-Gly-Tyr Complex at  $-509$  ppm by  $^{51}\text{V}$  NMR<sup>a</sup>



	ligand <sup>b</sup>	complex	$\Delta\delta$
C1	43.3	49.5	6.2
C2	169.2	181.1	11.9
C3	59.5	69.4	9.9
C4	180.6	183.6	3.0
C5	39.3	38.9	0.4
C6	132.1	131.1	1.0
C7	133.2	133.7	0.5
C8	118.1	117.9	0.2
C9	156.9	157.1	0.2

<sup>a</sup> 180 mM total vanadate, 32 mM Gly-Tyr, 24 h of incubation at 297 K pH 7.1 ( $\pm 0.1$ ). The spectroscopic parameters are specified in the Experimental Section. <sup>b</sup> The chemical shifts of the free ligand were confirmed in a  $^{13}\text{C}$  NMR spectrum of 148 mM Gly-Tyr at pH = 7.0 ( $\pm 0.1$ ).

emerge as the pH is increased from 8.5 to 10.5 in samples incubated for 10 days (Figure 2) and in a solution heated to 40 °C for 5 h.  $^{51}\text{V}$  NMR spectra of such solutions show up to five different signals in the presence of vanadate and oxygen. Only the reaction between vanadate and Gly-Ser has previously shown the formation of more than two complexes ( $-494$ ,  $-505$ , and  $-507$  ppm);<sup>8,9</sup> two of the vanadium(V)-Gly-Ser complexes involve coordination of the hydroxyl group on the serine side chain to the vanadium. Given the redox reactivity of tyrosine, and previous reports of metal ion catalyzed oxidations of tyrosine,<sup>29</sup> the nature of the additional species were examined in solutions in which oxygen had rigorously been excluded.

Solutions in which oxygen had rigorously been excluded generated  $^{51}\text{V}$  NMR spectra containing the major  $-509$  ppm signal and the minor  $-558$  ppm signal at 10–20 fold at excesses of Gly-Tyr. These solutions were colorless to faint yellow and remained colorless even after 2 weeks of incubation (or after heat treatment), in contrast to the yellow-brownish colors of solutions incubated in the presence of oxygen. On the basis of these experiments, we conclude that the  $-498$  ppm complex, despite its prevalence at high pH, is generated by vanadate-catalyzed Gly-Tyr oxidation and that the other observed resonances may also be derived from oxidation products. Further information concerning the  $-498$  ppm species will be presented below.

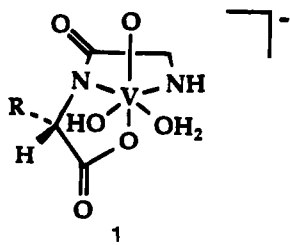
**$^{13}\text{C}$ ,  $^{15}\text{N}$ , and  $^{51}\text{V}$  NMR Spectroscopic Studies to Characterize the V-Gly-Tyr Complex at  $-509$  ppm.** The  $^{13}\text{C}$  NMR spectrum of a solution containing the complex at  $-509$  ppm was recorded at pH 7.10 ( $\pm 0.05$ ). The chemical shifts of all the carbons in the complex as well as the free ligand were identified and are reported in Table 2. Four carbon resonances in the complex show significant shifts from the free ligand: the carboxylate carbon (3.0 ppm), the carbonyl carbon in the amide group (11.9 ppm), the  $\text{CH}_2$  in the tyrosine (9.9 ppm), and the  $\text{CH}_2$  in the glycine (6.2 ppm). In addition, the carbons in the tyrosine side chain show small shifts ( $< 1$  ppm). On the basis of these data we conclude that the glycine  $\text{NH}_2$  group, the

(29) (a) Kitajima, N.; Koda, T.; Iwata, Y.; Moro-oka, Y. *J. Am. Chem. Soc.* **1990**, *112*, 8833–8839. (b) Harris, W. R.; Bess, Robert C.; Martell, A. E.; Ridgway, T. H. *J. Am. Chem. Soc.* **1977**, *99*, 2958–2963. (c) Maskos, Z.; Rush, J. D.; Koppenol, W. H. *Arch. Biochem. Biophys.* **1992**, *296*, 521–529.

peptide nitrogen (N(peptide)), and the carboxylate are all directly linked to the vanadium. The  $^{13}\text{C}$  chemical shifts of the phenol ring support the expectation that this moiety is not directly coordinated to the vanadium. The large chemical shifts of the amido carbonyl and the  $\text{CH}_2$  in the tyrosine residue contrasts with the smaller chemical shifts of the carbon in the  $\text{CH}_2\text{NH}_2$  and the carboxylate group. The involvement of the amide nitrogen is further supported by a 66 ppm downfield shift of the  $^{15}\text{N}$  NMR signal in the complex formed with the Gly– $^{15}\text{N}$ –Tyr (at 190 ppm). This  $^{15}\text{N}$  signal broadened upon complexation to a half-width of 42 Hz. These findings are consistent with deprotonation of the amide nitrogen in the complex.

The involvement of the tyrosine carboxylate was further confirmed by the reaction of vanadate with Gly–Tyr–amide. In this reaction no complex was observed at either –509 ppm or –498 ppm. Substitution of a proton with an alkyl group on the amide nitrogen prevented complex formation at –509 ppm.<sup>8,9</sup> The involvement of the glycine amino group in complex formation was explored using both (CBZ–Gly–Tyr) and  $^{15}\text{N}$  NMR. No complex was formed at –509 ppm when Gly–Tyr was protected, suggesting the amino group is necessary for formation of this complex. This is in contrast to the  $^{51}\text{V}$  NMR resonance at –498 ppm which forms in solutions containing vanadate and CBZ–Gly–Tyr. The  $\text{NH}_2$  involvement in the –509 ppm complex was examined by recording the  $^{15}\text{N}$  NMR spectrum of a solution containing 135 mM vanadate and 180 mM  $^{15}\text{N}$ – $\text{H}_2\text{N}$ –Gly–Tyr at pH 7.0 and compared this to a spectrum containing only ligand. The  $^{15}\text{N}$  signal for the  $^{15}\text{N}$ – $\text{H}_2\text{N}$ –Gly–Tyr at 27 ppm shifted to 16 ppm in the presence of vanadate. The observed shift supported the possibility that the nitrogen is indeed directly coordinated to the vanadium, and the chemical shift of free ligand at pH 8.4 supports an upfield shift upon deprotonation. The  $^{15}\text{N}$  signal associated with the complex is significantly line broadened ( $\Delta_{1/2} = 201$  Hz) as expected when the nitrogen is directly coordinated to the vanadium.

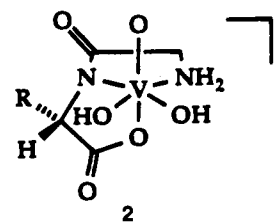
The major –509 ppm V–Gly–Tyr complex probably involves the amine group, the amide nitrogen and the carboxylate oxygen.<sup>8,9</sup> One type of vanadate–dipeptide complexes were previously proposed for the V–Gly–Ser complex (1).<sup>8</sup> In order to have a –OH and a –OH<sub>2</sub> group and be consistent with the reported pH dependence for complex formation, structure 1 will have both a deprotonated amide nitrogen ( $\text{CON}^-$ ) and a deprotonated amine (NH) nitrogen (detail not specified in original publication). In structure 1 the three oxygens (=O, –OH, or –OH<sub>2</sub>) not bound to the ligand could appear in any configurational arrangement, but only one form has been illustrated here. It should be noted that the oxygen atoms are expected to be different in the illustrations of these compounds, however, should the electron density be similar, the protons must be redistributed accordingly.



The large shift in the  $^{13}\text{C}$  upon complexation supports a very strong interaction of the amide nitrogen with the vanadium. These observations are consistent with a deprotonated amide nitrogen. Solid state and solution studies confirm the loss of the amide proton in various other metal complexes.<sup>20–26</sup>

Formation of similar peptide complexes from metal ions such as  $\text{Cu}^{2+}$ ,  $\text{Ni}^{2+}$ , and  $\text{Pb}^{2+}$  can be slow, presumably because the amide is fairly difficult to deprotonate in aqueous solutions. The reaction of Gly–Tyr with vanadate yield rates which are consistent with slow deprotonation of the amide proton. The product at –509 ppm is not observed if the terminal amine group is protected by a CBZ group, whereas a product is formed when vanadate and Pro–Gly are mixed.<sup>8</sup>  $^{13}\text{C}$  chemical shifts show the carbon  $\alpha$  to the nitrogen shifts on coordination to the vanadium but not as far as the amide carbon. These observations are therefore consistent with a coordinative bond between the lone pair of the terminal amino group and the vanadium atom.

With the requisite removal of the amide nitrogen proton and the coordinative bond between the terminal amine and the vanadium, we revise the proposed structure 1 to 2, each of which has a charge of 1–. Although octahedral coordination has not been strictly proven, the solution studies available on related systems suggest octahedral coordination around the vanadium (perhaps with one exception<sup>12b</sup>).<sup>9,13,16,31,32</sup> The small  $^{13}\text{C}$  shift of the carboxylate carbon upon complexation suggests that the carboxylate interactions may be fairly weak by virtue of a trans effect induced by the oxo ligand and thus axial in the complex as shown in 2. Such a pattern was observed for oxovanadium(V) triethanolamine, oxovanadium(V) (*S,S,S*)-triisopropanolamine and oxotris(pivalato)vanadium, all of which have been characterized in solution and in the solid state.<sup>31</sup> The  $^{13}\text{C}$  NMR data is in agreement with structure 2.



In addition to the octahedral complex 2, an analogous pentacoordinate complex (generated by losing an  $\text{OH}^-$  from structure 2) can also be proposed. The  $^{13}\text{C}$  and  $^{51}\text{V}$  NMR data and geometry of the ligand are less supportive of the five-coordinate structure than of 2.<sup>32</sup>

#### Electrochemical Properties of the V–Gly–Tyr Complex.

The electrochemistry of solutions containing 1.0 mM vanadate and 3.0 mM Gly–Tyr in 0.2 M LiCl saturated with  $\text{N}_2$  at pH 7.0 and 8.3, respectively, was examined. Reversible redox waves were not found. In the pH 8.3 solution, an indication of an oxidation step was observed at ca. +0.5 V (relative SCE), which was not observed in solutions containing Gly–Tyr or vanadate, respectively. A solution of tyrosine also did not show redox activity from +0.8 to –0.8 V. We conclude that the V–Gly–Tyr may be redox active in the voltage range examined.

- (30) (a) Boas, L. V.; Pessoa, J. C. *Comprehensive Coordination Chemistry*; Wilkinson, G., Gillard, R. D., McCleverty, J. A., Eds.; Pergamon Press: New York, 1987; Vol. 3, p 453–584. (b) Pessoa, J. C.; Antunes, J. L.; Boas, L. F. V.; Gillard, R. D. *Polyhedron* **1992**, *11*, 1449–1461.
- (31) (a) Crans, D. C.; Chen, H.; Anderson, O. P.; Miller, M. M. *J. Am. Chem. Soc.* **1993**, *115*, 6769–6776. (b) Rehder, D.; Priebisch, W.; von Oeynhausen, M. *Angew. Chem., Int. Ed. Engl.* **1989**, *28*, 1221–1222.
- (32) (a) Crans, D. C.; Shin, P. K. *J. Am. Chem. Soc.* **1994**, *116*, 1305–1315. (b) Crans, D. C.; Shin, P. K.; Armstrong, K. B. *Mechanistic Bioinorganic Chemistry*; Thorp, H., Ed.; American Chemical Society: Washington, DC, 1995; in press. (c) Amos, L. W.; Sawyer, D. T. *Inorg. Chem.* **1972**, *11*, 2692–2697.

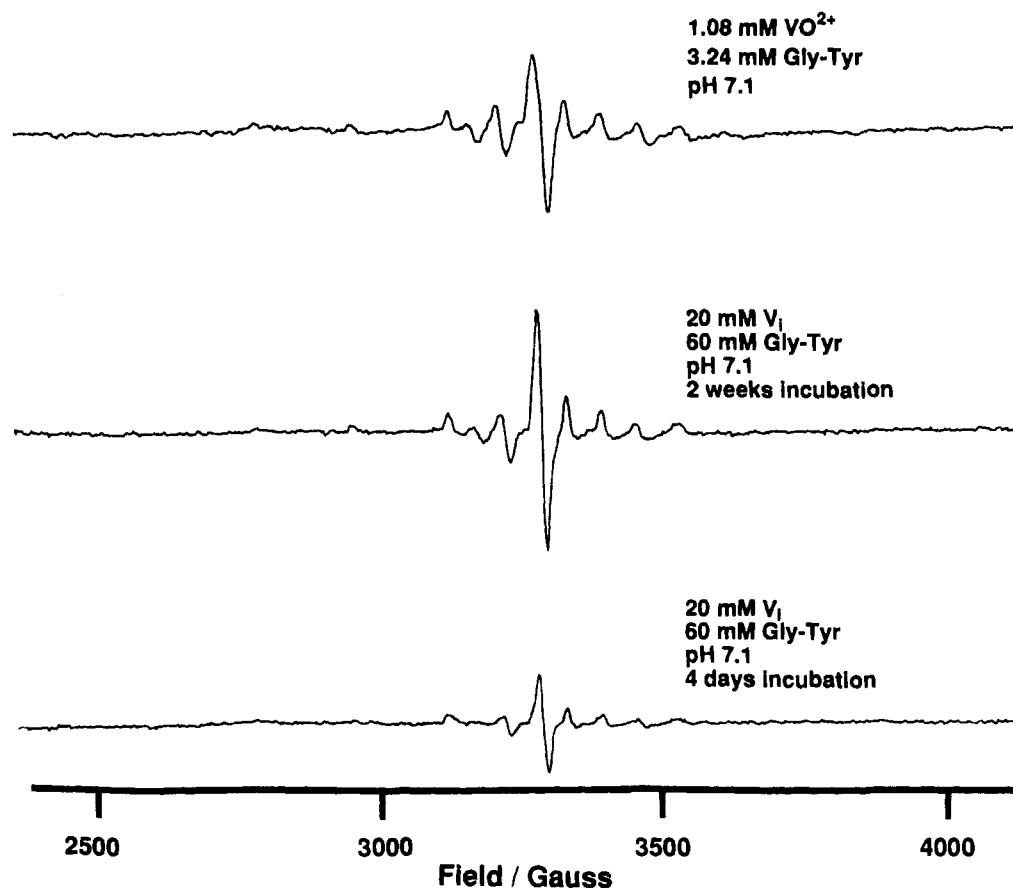


**Figure 3.** EPR spectra of solutions containing 20 mM vanadate and 80 mM Gly-Tyr in the presence of oxygen shown at pH 7.1 after four days of incubation (bottom) and at pH 7.1 after two weeks of incubation (center). The top EPR spectrum is obtained for a solution containing 1.08 mM vanadyl sulfate and 3.24 mM of Gly-Tyr at pH 7.1. Thirty scans were acquired for the center and bottom spectra, whereas only one scan was acquired for the top spectrum.

#### Spectroscopic Characterization of the Gly-Tyr Oxidation by Vanadate in the Absence and Presence of Oxygen.

Experiments by both EPR and  $^{51}\text{V}$  NMR spectroscopy were carried out on two series of solutions at pH 7.1 and at pH 8.1. One series of solutions (20 mM vanadate and 60 mM Gly-Tyr) were prepared rigorously in the absence of oxygen (see Experimental Section), and the other series under the conditions similar to those used for the studies described in this manuscript (that is, the solutions were protected from microorganism contamination, but not from oxygen). The EPR spectrum obtained after four days show a weak signal (Figure 3, bottom) which increases upon further incubation (Figure 3, center). Even after two weeks of incubation only little reduction of the vanadate (in the form of  $0.22 (\pm 0.02)$  mM  $\text{VO}^{2+}$ -Gly-Tyr) was observed by EPR spectroscopy in the solution containing 20 mM vanadate and 60 mM Gly-Tyr in the absence of oxygen. The sample incubated in the presence of oxygen showed similar ( $0.21 (\pm 0.01)$  mM  $\text{VO}^{2+}$ -Gly-Tyr) reduction after two weeks of incubation. The pH of the samples was monitored during the incubation period, and if necessary, was adjusted. The color of the solution incubated in the presence of oxygen had changed from colorless to faint yellow after 2 weeks. The facts no major differences were found between the vanadium(IV) concentrations of the samples incubated in the presence and absence of oxygen, and significantly more  $-498$  ppm signal was observed in the solution incubated in the presence of oxygen, demonstrate that all the vanadium(IV) formed by reduction does not accumulate as the  $\text{VO}^{2+}$ -Gly-Tyr species in this solution.

The nature of the species formed in solution was examined by recording the EPR spectrum of a solution containing 1.08 mM vanadyl sulfate and 3.24 mM Gly-Tyr at acidic pH ( $\sim 4$ )

and neutral pH ( $\sim 7$ ). At pH 4 the characteristic vanadyl cation spectrum was observed unless the solutions had been incubated for some time. The spectrum obtained from faint yellow solution of vanadyl cation and Gly-Tyr at pH 7 (Figure 3 top) is identical to that obtained from  $\text{V}_i$  and Gly-Tyr. Combined, these studies are consistent with the possibility that the vanadate oxidized the Gly-Tyr formed a  $\text{VO}^{2+}$ -Gly-Tyr complex and eventually was reoxidized by oxygen to vanadium(V) complexes. A solution containing 20 mM  $\text{V}_i$  and 60 mM Gly-Tyr incubated for 3 weeks was used to record an EPR spectrum that allowed us to derive the parameters for the  $\text{VO}^{2+}$ -Gly-Tyr complex. As reported previously, a series of vanadyl complexes forms in the solution of amino acids and simple peptides.<sup>30</sup> The parameters for this complex obtained for  $g_{\parallel}$  and  $A_{\parallel}$  are 1.941 and  $-166 \times 10^{-4} \text{ cm}^{-1}$ , and for  $g_{\perp}$  and  $A_{\perp}$  are 1.985 and  $-52 \times 10^{-4} \text{ cm}^{-1}$ , respectively.

Incubation of the colorless solution containing 20 mM vanadate and 60 mM peptide at pH 8.1 (and higher pH) prepared in the absence of oxygen was faint yellow after two weeks of incubation. Surprisingly, the EPR signal of this sample ( $0.19 (\pm 0.02)$  mM of  $\text{VO}^{2+}$ -Gly-Tyr) was of similar magnitude as the spectrum observed at pH 7.1 after two weeks of incubation. No resonance was observed at  $-498$  ppm in these solutions in contrast to the solution incubated in the presence of oxygen. These observations are consistent with the signals at  $-498$  ppm being a result of Gly-Tyr oxidation and that the  $\text{VO}^{2+}$ -Gly-Tyr complex readily reoxidizes. Indeed, variable concentrations of the  $-498$  ppm signal was observed at pH 8.1 and higher pH depending on the exact treatment of the solution (presence of oxygen, heating cycles or incubation times).

#### Time Dependence of Vanadate-Gly-Tyr Complex For-

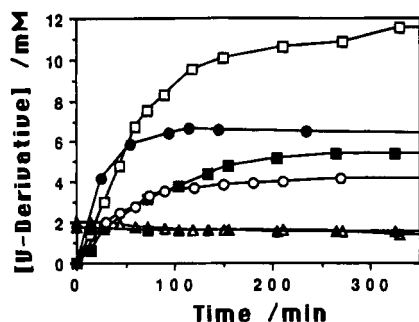


**Figure 4.** Concentration of the major vanadate-peptide complex ( $-509$  ppm) in 20 mM vanadate at 300 K followed as a function of time. The symbols used and equilibrium concentrations shown are as follows:  $[V-Gly-Tyr]$  (■) (5.4 mM) and  $[V_1]$  (▲) (1.54 mM) in solutions with 40 mM Gly-Tyr at pH 7.10,  $[V-Gly-Tyr]$  (□) (11.9 mM) and  $[V_1]$  (△) (1.4 mM) in solutions with 60 mM Gly-Tyr at pH 7.10,  $[V-Gly-Tyr]$  (○) (4.25 mM) and  $[V_1]$  (●) (1.98 mM) in solutions with 60 mM Gly-Tyr at pH 8.40, and  $[V-Gly-Ser]$  (●) (6.42 mM) in solutions with 60 mM Gly-Ser at 7.10.

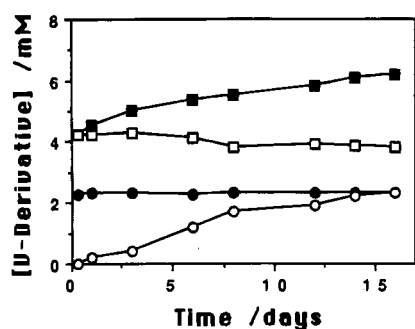


**Figure 5.** Concentration of the two V-Tyr-Gly complexes determined as a function of time. The concentrations for the total complex (■), the complex at  $-509$  ppm (□), the complex at  $-498$  ppm (○) and  $V_1$  (●) are shown.

**mation.** The concentration of V-Gly-Tyr complex ( $-509$  ppm) in 20 mM vanadate with both 40 mM and 60 mM Gly-Tyr at pH 7.1 and 300 K as a function of time (in the presence of oxygen) is shown in Figure 4. The complex forms steadily during the first hours of reaction and approaches an equilibrium mixture after 4–5 h. The initial rate of complex formation was approximated from the complex formation shown in Figure 4. During the initial period of complex formation, the concentration of vanadate monomer decreases as the complex concentration increases. Whether the slow complex formation is limited to the V-Gly-Tyr complex was explored by measuring the formation of vanadium(V)-Gly-Ser complex as a function of time (Figure 4). The formation of the V-Gly-Ser complex was slightly faster than the formation of the V-Gly-Tyr complex, approaching equilibrium after 1–2 h.

The reaction of 20 mM vanadate with 60 mM Gly-Tyr at pH 8.4 and 300 K was also followed (Figures 4 and 5). The formation of the  $-509$  ppm signal at higher pH is slower than the complex formation at lower pH. The complexes at  $-498$  and  $-505$  ppm form significantly more slowly than the  $-509$  ppm complex, consistent with the possibility that both may be decomposition products. The  $-498$  ppm complex appeared after the formation of the  $-509$  ppm complex. Whether the  $-498$  ppm complex formed directly from vanadate and peptide or from the  $-509$  ppm complex cannot be determined with certainty from these studies, although the observed lag phase would support the interpretation that the  $-498$  ppm complex formed from the  $-509$  ppm complex.

To further characterize the new resonance at  $-498$  ppm, we recorded UV spectra of solutions containing this species and

compared the absorption spectra to those observed from solutions containing the  $-509$  ppm complex and vanadate. No new distinctive absorption maxima were apparent even though increased absorption at longer wavelengths was observed. Similar absorption spectra have previously been reported for metal-catalyzed oxidation products of (3,4-dihydroxyphenyl)-alanine solutions.<sup>29c</sup>

$^1H$  NMR spectra were recorded at various stages during the incubations to determine if the Gly-Tyr ligand indeed was oxidizing. After a few days of incubation at pH 9.1, some changes were observable both in the  $^1H$  and  $^{51}V$  NMR spectra consistent with V-Gly-Tyr complex formation. However, as the incubation time increased, conversion of the free Gly-Tyr becomes apparent in the  $^1H$  and the  $^{13}C$  NMR spectra. Since the  $-498$  ppm signal becomes the dominant resonance in the  $^{51}V$  NMR spectrum and the  $^{13}C$  NMR spectra show many new resonances, it is likely that the  $-498$  ppm resonance in the  $^{51}V$  NMR spectrum consists of a composite of vanadium(V)-Gly-Tyr-oxidation products. We conclude that Gly-Tyr is being oxidized, and since only low levels of EPR signals are observed at any point in time, the vanadium(IV) formed upon Gly-Tyr oxidation is recycled to vanadium(V) in these solutions.

#### The Rate Law and Rate Constants of Complex Formation.

Measuring the rate of complex formation at various concentrations of peptide, vanadate, and  $H^+$  will allow determination of the rate law. The rate of complex formation was measured at constant total vanadate and dipeptide concentration at constant pH using  $^{51}V$  NMR spectroscopy. Recording the spectra at given time points after beginning the reaction, integrating the spectra and using the mole fraction for each vanadium species the concentration of each species was calculated. The rate is then obtained by converting the observed concentration of complex to the concentration that formed per time unit. First, the proportionality between the rate and each of the vanadate monomer and peptide concentration was demonstrated by measuring the rates in solutions where one component was kept constant and the other varied at constant pH (data not shown). This is consistent with a rate law dependent on both  $[V_1]$  and  $[Gly-Tyr]$  where the protonation state has not been specified for  $V_1$  or Gly-Tyr.

Through rapid protonation and deprotonation reactions, several pathways are kinetically indistinguishable<sup>33</sup> and this will be discussed below. First, we consider several species that can contribute to the reaction rate, and define a general rate equation for complex formation which includes terms for the two vanadate anions  $H_2VO_4^-$  and  $HVO_4^{2-}$  and the zwitterion (Gly-Tyr<sup>z</sup>) and the anionic form (Gly-Tyr<sup>-</sup>) of the dipeptide in solution, (9). In (9)  $k_1$ ,  $k_2$ ,  $k_3$ , and  $k_4$  are the specific rate constants for each composite pathway. Each contribution described in the rate terms is not an elemental reaction (for example,  $[H^+]^{-1}$  may be indicative of base catalysis or reaction of the deprotonated vanadate monomer). However, this approach describes the overall rate so that we can begin to identify and consider the major and minor pathways. Substituting  $[HVO_4^{2-}] = [H_2VO_4^-] K_{aH_2VO_4}/[H^+]$  and  $[Gly-Tyr^z] = [Gly-Tyr^-] [H^+]/K_{aGly-Tyr}$  into (9) gives (10). None of the rate constants in (10) exceed that defined by the diffusion limit, and since the reaction is studied in aqueous solution in the pH range 6–10,  $[H^+]$  is finite. Plotting rate/ $[Gly-Tyr^-]$  as a function of  $[H_2VO_4^-]$  for a series of measurements at constant pH gives a linear relationship where the slope represent the combined

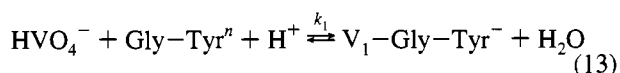
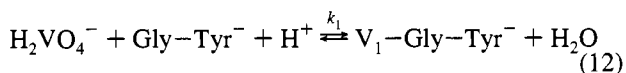
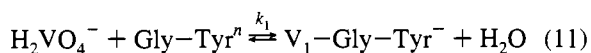


rate constants as defined by (10) (data not shown).

$$\begin{aligned} d[\text{V-Gly-Tyr}]/dt = & [\text{H}_2\text{VO}_4^-](k_1[\text{Gly-Tyr}^n] + \\ & k_2[\text{Gly-Tyr}^-]) + [\text{HVO}_4^{2-}](k_3[\text{Gly-Tyr}^n] + \\ & k_4[\text{Gly-Tyr}^-]) \quad (9) \end{aligned}$$

$$\begin{aligned} d[\text{V-Gly-Tyr}]/dt = & [\text{H}_2\text{VO}_4^-][\text{Gly-Tyr}^-]\{k_1[\text{H}^+]/K_{\text{aGly-Tyr}} + \\ & k_2 + k_3K_{\text{aH}_2\text{VO}_4^-}/K_{\text{aGly-Tyr}} + k_4K_{\text{aH}_2\text{VO}_4^-}/[\text{H}^+]\} \quad (10) \end{aligned}$$

In a second set of experiments the rate of complex formation was measured at varying pH. This series of measurements was carried out to examine the combination of the rate terms involving  $\text{HVO}_4^{2-}$ ,  $\text{H}_2\text{VO}_4^-$ ,  $\text{Gly-Tyr}^n$ ,  $\text{Gly-Tyr}^-$ , and  $\text{H}^+$  concentration. The contributions of each pathway can be determined in a study measuring rates at various pH values and constant overall vanadate and peptide concentrations. Plotting the observed rates in this study as a function of  $[\text{H}_2\text{VO}_4^-][\text{Gly-Tyr}^-]$ ,  $[\text{HVO}_4^{2-}][\text{Gly-Tyr}^n]$ , or  $[\text{HVO}_4^{2-}][\text{Gly-Tyr}^-]$  gives correlations with no physical meaning (a negative rate constant) and do not represent viable possibilities as the composite pathway for the major contributor. Plotting the rate as a function of  $[\text{H}_2\text{VO}_4^-][\text{Gly-Tyr}^n]$  gives a linear relationship with a positive rate constant. A similar linear relationship is obtained if the rate is plotted as a function of the kinetically indistinguishable pathways<sup>33</sup>  $[\text{HVO}_4^{2-}][\text{Gly-Tyr}^n][\text{H}^+]$  or  $[\text{H}_2\text{VO}_4^-][\text{Gly-Tyr}^-][\text{H}^+]$ . This finding suggests  $k_1$  and  $k_2$  and/or  $k_3$  in (10) will be significant contributors to the observed complex formation.



One pathway defined by the rate constant  $k_1$  is the reaction between  $\text{H}_2\text{VO}_4^-$  and  $\text{Gly-Tyr}^n$ , (11). A second kinetically indistinguishable pathway for complex formation described by this rate term is the reaction of  $\text{H}_2\text{VO}_4^-$  with  $\text{Gly-Tyr}^-$  under acid catalysis, (12). A third indistinguishable pathway for complex formation described by this rate term is the reaction of  $\text{HVO}_4^{2-}$  with  $\text{Gly-Tyr}^n$  under acid catalysis, (13). All three pathways should show increased rate upon increased concentration of each reaction component. Since a plot of the rate divided by  $[\text{Gly-Tyr}^n]$  as a function of  $[\text{H}_2\text{VO}_4^-]$  or  $[\text{HVO}_4^{2-}][\text{H}^+]$  gave a linear relationship with a negative slope, the first and the third mechanisms can be eliminated. The reaction of  $\text{H}_2\text{VO}_4^-$  with  $\text{Gly-Tyr}^-$  which is governed by a rate-limiting step involving  $\text{H}^+$  transfer is the most likely pathway responsible for V-Gly-Tyr formation. Plotting the  $d[\text{V-Gly-Tyr}]/d[\text{H}_2\text{VO}_4^-][\text{Gly-Tyr}^-]$  as a function of  $[\text{H}^+]$  gives a linear relationship (Figure 6). Since  $k_1$  is the rate constant defining this pathway, the rate constant of interest was calculated from the slope ( $k_1 = \text{slope} \times K_{\text{aGly-Tyr}}$ ) of Figure 5 to be  $1.0 (\pm 0.1) \text{ M}^{-2} \text{ min}^{-1}$  ( $0.017 (\pm 0.002) \text{ M}^{-2} \text{ s}^{-1}$ ).

The reaction of  $\text{H}_2\text{VO}_4^-$  with  $\text{Gly-Tyr}^-$  can occur both with ( $k_1$ ) and without ( $k_2$ ) acid catalysis. Additionally,  $\text{HVO}_4^{2-}$  can react with  $\text{Gly-Tyr}^-$  ( $k_3$ ) with and without ( $k_4$ ) acid catalysis. It is also possible to interpret the pathway described by  $k_4$  as base catalysis. No evidence for the pathway involving  $\text{HVO}_4^{2-}$

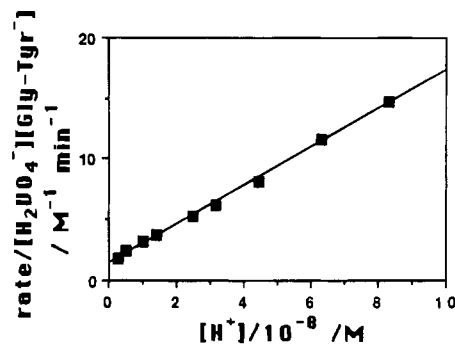
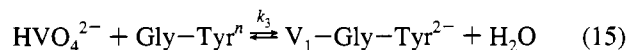
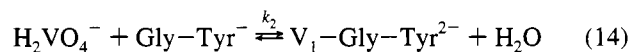


Figure 6. Rate of V-Gly-Tyr complex ( $-509$  ppm) formation divided by  $[\text{H}_2\text{VO}_4^-][\text{Gly-Tyr}^-]$  plotted as a function of  $10^8[\text{H}^+]$ .

with  $\text{Gly-Tyr}^-$  as represented by the rate constant  $k_4$  was observed at these pH. From the intercept in Figure 6 a combined rate constant of  $k_2 + k_3K_{\text{aH}_2\text{VO}_4^-}/K_{\text{aGly-Tyr}}$  of  $1.5 (\pm 0.1) \text{ M}^{-1} \text{ min}^{-1}$  ( $0.025 (\pm 0.003) \text{ M}^{-1} \text{ s}^{-1}$ ) was calculated. The pathways involving  $\text{Gly-Tyr}^-$  and  $\text{H}_2\text{VO}_4^-$ , (14), or  $\text{Gly-Tyr}^n$  and  $\text{HVO}_4^{2-}$ , (15), are kinetically indistinguishable in these measurements. This is in part due to the similarity of  $\text{p}K_{\text{a}}$ 's for  $\text{H}_2\text{VO}_4^-$  (8.2) and  $\text{Gly-Tyr}^n$  (8.2) under these conditions. However,  $\text{H}_2\text{VO}_4^-$  is a better electrophile than  $\text{HVO}_4^{2-}$  by a factor of  $1000^{34}$  and  $\text{Gly-Tyr}^-$  is a better nucleophile than  $\text{Gly-Tyr}^n$ , so  $k_2$  is likely to be a greater contributor to the overall rate than  $k_3$ . This argument is supported by the observation that the reaction of  $\text{HVO}_4^{2-}$  with a good nucleophile  $\text{Gly-Tyr}^-$  (in comparison with  $\text{Gly-Tyr}^n$ ) defined by the rate constant  $k_4$  is insignificant in the pH range from 7.0 to 8.6. An upper limit for the rate constant  $k_2$  is therefore  $1.5 (\pm 0.1) \text{ M}^{-1} \text{ min}^{-1}$  ( $0.025 (\pm 0.003) \text{ M}^{-1} \text{ s}^{-1}$ ) (14), which would be accompanied by an insignificant and small  $k_3$  (15).



The second order rate constant ( $k_2$ ) is significantly lower than those previously reported for the vanadate dimerization reaction based on the reaction between  $\text{H}_2\text{VO}_4^-$  and  $\text{HVO}_4^{2-}$ .<sup>29,34,35</sup> Rate constants for the formation of various vanadate complexes including vanadium(V)-Tricine,<sup>16</sup> vanadium(V)-alizerin,<sup>17</sup> and vanadium(V)-EDTA<sup>17</sup> complexes all have rate constants of similar magnitude ( $10^4 \text{ M}^{-1} \text{ s}^{-1}$ ). The V-Gly-Tyr complex may distinguish itself from the rapidly formed complexes because of its deprotonated amide nitrogen-vanadium(V) bond. In light of the greater stability of the V-Gly-Tyr complex, we discuss possible mechanisms of formation.

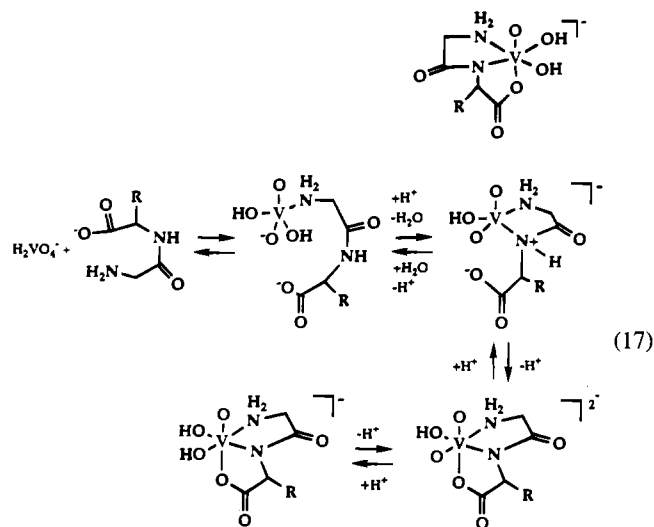
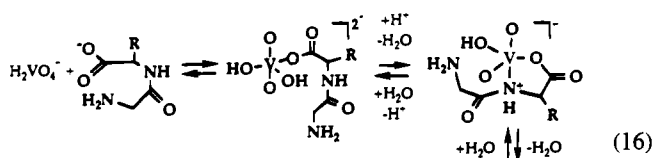
**Mechanisms of V-Gly-Tyr Complex Formation.** Two mechanisms for the formation of the  $-509$  ppm complex consistent with the rate data produced by the rate constant  $k_1$  are shown in (16) and (17). In both mechanisms,  $\text{H}_2\text{VO}_4^-$  reacts with  $\text{Gly-Tyr}^-$  and the rate-limiting step involves  $\text{H}^+$  catalysis. In the first mechanism, (16), we show the initial attack by the carboxylate group, whereas the second mechanism shows the initial attack by the amine group, (17).

Several reasonable modifications and alternative mechanisms can be proposed but only two are shown here. They illustrate the types of reactions that are involved when generating the

(34) Crans, D. C.; Rithner, C. D.; Kustin, K.; Theisen, L. A. Manuscript in preparation.

(35) Whittaker, M. P.; Asay, J.; Eyring, E. M. *J. Phys. Chem.* **1966**, *70*, 1005-1008.

(36) Kustin, K.; Liu, S.-T.; Nicolini, C.; Toppen, D. L. *J. Am. Chem. Soc.* **1974**, *96*, 7410-7415.



complex defined by the rate constant  $k_1$ . Each of these mechanisms must contain one or more proton transfer steps which have the potential of being rate-limiting. The reaction illustrated in (16) is initiated by attack from the carboxylate which is followed by coordination of the amide nitrogen and loss of a proton. In other peptide–metal ion complexes, once the amide nitrogen is protonated, the complex is believed to fall apart.<sup>20b</sup> Alternatively, it is possible the amide nitrogen loses its proton first in various ways before coordination to the vanadium. The last step involves coordination of the amine to the vanadium. Although the V–Tricine complex is likely to form through a dissociative pathway,<sup>16</sup> the sequential approach by the multidentate ligands to the vanadium is likely to take place through similar steps as shown in (16) (or (17)). The V–Tricine complex has the hydroxyl groups dissociating from the metal while the carboxylate remains bound as evidenced by cross peaks in a 2D <sup>13</sup>C EXSY spectrum.<sup>16</sup>

The mechanism shown in (17) is initiated by attack of the terminal amino group which in the deprotonated form is the most nucleophilic moiety of the dipeptide. Evidence for this type of reaction has not previously been reported with ligands containing oxygen ligating moieties. Unfortunately, the time-scale of this reaction is not appropriate to obtain similar evidence by multinuclear EXSY spectroscopy. However, the rate law requires that the rate-limiting step involves a proton transfer step. The second step presumably involves a proton transfer from the solvent to facilitate the amide nitrogen bond formation; then the carboxylate chelates to the vanadium and proton transfer completes the complex formation. Since it is difficult to deprotonate the amide nitrogen, this step may be initiated by the loss of a water molecule followed by bond formation between a protonated amide nitrogen and the vanadium; the rate-limiting step has previously been attributed to loss of a water molecule.<sup>17</sup> Alternatively, the rate-limiting step in both mechanisms 16 and 17 may involve tautomerization and chelation of the amide which will lead to loss of the amide proton.

The reaction determined by the rate constant  $k_2$  does not involve a proton in the rate-limiting step. Accordingly, the one possible mechanism shown in (18) describes a reaction in which the first step is attack by the carboxylate, coordination by the

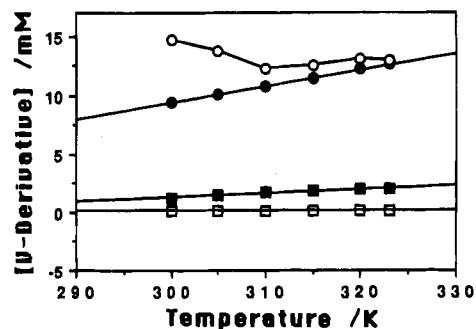
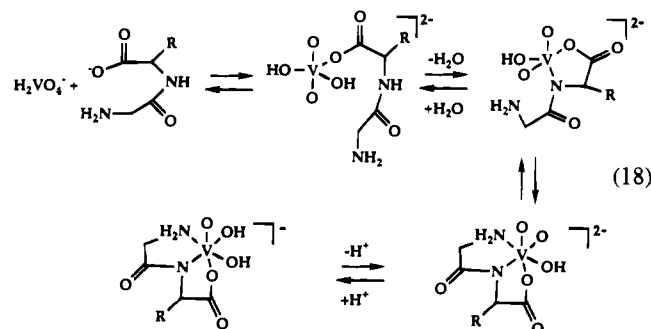


**Figure 7.** Concentration of V–Gly–Tyr complex (–509 ppm) (●) and V<sub>1</sub> (■) in a sample containing 20 mM total vanadate and 60 mM total Gly–Tyr as shown as a function of temperature. The values for 100K<sub>eq</sub> (○) and K<sub>eq</sub> (□) are also shown.

amide nitrogen while immediately losing the proton (corresponding to (16) without the acid catalysis). A similar mechanism can be proposed with the amine group initiating complex formation (not shown). The rate constants for the acid catalyzed and the uncatalyzed reactions are of similar magnitude. At most pH values in the physiological range, the acid-catalyzed reaction contributes less to the overall reaction than the acid independent reaction. The fact that H<sub>2</sub>VO<sub>4</sub><sup>–</sup> and Gly–Tyr<sup>–</sup> both are reactants guarantees that this reaction will have a small pH window with significant rates of formation since only at these pH are the reactants in the appropriate form.



**Effect of Temperature on the Vanadate Reaction with Gly–Tyr.** To examine the effect of sample preparation on the measured formation constants of V–Gly–Tyr we measure K<sub>eq</sub> in samples prepared by a procedure that involved three periods of heating with adjustment to the pH, followed by five days incubation at ambient temperature. As shown in Table 1, we obtained identical formation constants within experimental error relative to those involving no heating and incubation for 5 days before recording NMR spectra. A sample containing 20 mM vanadate and 60 mM Gly–Tyr at pH 7.1 was also examined at various temperatures. The sample was incubated for a minimum of 5 h at the desired temperature before the <sup>51</sup>V NMR spectrum was recorded. As shown in Figure 7 the concentration of V–Gly–Tyr complex increases significantly at higher temperatures. The concentration of vanadate monomer also increases significantly at the higher temperatures. As a consequence, the K<sub>eq</sub> for the V–Gly–Tyr complex is essentially constant despite the large increase in V–Gly–Tyr.

In the past, the vanadate solutions have been heated to ensure no decameric vanadate is present in solution;<sup>3b,9,11,12</sup> we here caution that such heating treatments be used carefully since they could result in formation of high levels of complexes that only slowly hydrolyze at ambient temperature. If a solution of V<sub>1</sub> and Gly–Tyr is heated, a high concentration of the V–Gly–Tyr complex will form along with a high vanadate monomer concentration. When this solution is cooled to ambient tem-

peratures, the high V–Gly–Tyr concentration will only slowly reach the lower equilibrium concentration, whereas the vanadate oligomers will rapidly equilibrate. As a result, artificially high formation constants could be measured if inappropriate incubation periods are employed. Furthermore, such treatments will support higher levels of redox chemistry.

The increase in complex formation at higher temperatures is important for several reasons. First, this finding suggests these complexes are very sensitive to temperature, and accordingly, chemical and biological studies may show variations unless the temperature is maintained constant. Second, preparations of samples using a method involving several heat treatments are very likely to result in samples showing artificially high complex concentrations, because the equilibrium was established at higher pH and it will take extended time periods to obtain true equilibrium conditions. Heat treatments are recommended to eliminate the decamer component in vanadate solutions; however, such treatments can be treacherous. Last, but not the least, the potential for redox chemistry significantly increases at higher temperatures. However, higher concentrations of complexes at elevated temperatures (in the absence of redox chemistry) may facilitate studies of complexes that could only be conducted with difficulty at lower concentrations.

The increased formation of the vanadate–dipeptide complex at higher temperatures is significant with regard to the concentration of vanadium required to induce a particular biological response. In most systems reported to date, the interactions of vanadium with biomolecules occurs rapidly, and thus the effects of the increased temperature in mammals should result in a somewhat higher concentration of active complex. However, the studies with vanadate and Gly–Tyr or Gly–Ser suggest that other dipeptides may show slow formation rates as well. Such a time delay may be important for interactions of vanadate *in vivo*, and in part may be responsible for a possible lag-time before symptoms of vanadium administration are apparent. A biological system may be able to accommodate a much greater dose of vanadium than acceptable to the organisms because the vanadium already inside the organisms has neither the requisite amount of time nor the proper temperature to form the complex that would eventually result in a biological response and prevent additional vanadium from entering the cell. Whether such complexes play a role in biological systems still remains to be determined, particularly since many vanadium(V) compounds will be reduced to vanadium(IV) in a cellular environment.

## Conclusion

The major vanadium(V)–Gly–Tyr complex is found to form and hydrolyze much slower in aqueous solutions than similar ethanolamine-derived complexes. The formation of the vanadium(V)–Gly–Ser complex also takes more than one hour to establish equilibrium. It appears the deprotonated amide nitrogen moiety in the complex may be responsible for the higher stability. Temperature will increase the equilibrium concentrations of complex significantly, however, the vanadate monomer concentration also increases such that in the case of the vanadium(V)–Gly–Tyr,  $K_{\text{eq,V-Gly-Tyr}}$  is invariant as a function of temperature. Upon prolonged incubations, oxidation of the Gly–Tyr was observed in these solutions, and vanadium(IV) products at the 1% level were measured by EPR spectroscopy. No differences were observed in formation of vanadium(IV) products whether oxygen was present or absent, suggesting that the vanadium(IV) compound upon formation was recycled to a vanadium(V) complex in the presence of oxygen. This was confirmed by  $^{51}\text{V}$  NMR spectroscopy that shows accumulation of a new major species at  $-498$  ppm upon extended incubations. The vanadium(V) complex was found to form through two mechanisms, involving  $\text{H}_2\text{VO}_4^-$  and deprotonated Gly–Tyr ( $\text{Gly-Tyr}^-$ ), one with and one without acid catalysis. The rate constant for the first pathway was  $0.017 (\pm 0.002) \text{ M}^{-2} \text{ s}^{-1}$  and the rate constant for the second pathway was  $0.025 (\pm 0.003) \text{ M}^{-1} \text{ s}^{-1}$ . Both these rate constants of formation are significantly smaller than several other vanadium complexes (V<sub>2</sub>, V–alizerin, V–Tricine, V–EDTA, V–Na<sup>+</sup>K<sup>+</sup>ATPase) that all have H<sup>+</sup> independent rate constants of formation in the range of  $10^4 \text{ M}^{-1} \text{ s}^{-1}$ . The vanadium(V)–peptide complexes may represent a group of vanadium-derivatives that have potential as hydrolytically stable vanadium derivatives which should be important considering the recent interest in vanadium-derived antidiabetic drugs.

**Acknowledgment.** We thank the NIH (to D.C.C.) and the Deutsche Forschungsgemeinschaft (to D.R.) for funding this research. We thank Dr. Robert W. Marshman for recording the 132 MHz  $^{51}\text{V}$  NMR spectra, Mr. Haojiang Chen for recording the  $^{15}\text{N}$  NMR spectra, and Dr. Paul K. Shin for stimulating discussions.

IC941445P